

Determination of segmental and overall ventilation of clothed walking human by means of electric circuit analogy

Textile Research Journal
2018, Vol. 88(5) 586–601
© The Author(s) 2016
Reprints and permissions:
sagepub.co.uk/journalsPermissions.nav
DOI: 10.1177/0040517516685284
journals.sagepub.com/home/trj


Naghham Ismail, Nesreen Ghaddar and Kamel Ghali

Abstract

A new simplified model has been developed to determine the ventilation induced by swinging motion and external wind for a fabric clothed cylinder representing a limb or a trunk. The simplified model is based on an analogy between air flow and an electric circuit. When a clothed body segment is subject to external wind, the microclimate air flow electric circuit is represented by resistances. When the clothed segment is subject to a swinging motion, the air flow electric circuit is composed of inductance and resistance elements. The model is validated by comparing the predicted ventilation rates to published experimental data in different conditions: varying permeability, wind speeds, swinging frequencies (for the clothed arm), walking conditions, and aperture configurations. The predictions of the simplified model lie within the standard deviation range of the published experiments. Moreover, although it is simplified, the relative error between the simplified model and the published experiment of an oscillating limb is considered acceptable (18%).

Keywords

microclimate ventilation, electric circuit analogy, clothing ventilation during walking

Determination of clothing ventilation has been the focus of many studies.^{1–3} Indeed, clothing microclimate ventilation has a major influence on thermal comfort and dynamic insulation values of clothing ensembles. This is due to the fact that clothing microclimate ventilation is critical to the removal of sensible and latent heat from the body to the environment.⁴ However, researchers have followed different methods to achieve this goal experimentally and by mathematical modeling. The experimental methods adopted have normally used the trace gas dilution method and have reported the average ventilation value for the clothed body surface area.^{5–10} On the other hand, mathematical modeling methods have proved their effectiveness in predicting the ventilation rates under different conditions. They have mainly been based on representing the human clothed segment by an inner cylinder representing the body skin and an outer cylinder representing the clothing.^{11–14} Afterwards, they solved the coupled momentum, mass, and heat balances inside the microclimate air layer between the outer and inner cylinders to determine local ventilation rates.

Different postures (standing or walking), external wind conditions, and clothing apertures were modeled

mathematically to estimate the ventilation rate. Some mathematical models have considered the ventilation rate through independent clothed segments, such as clothed trunk or limb, subjected to external wind.^{13,15} In these cases, the ventilation is essentially related to the flow characteristics in the microclimate air layer governed by clothing air permeability, air gap thickness, and clothing aperture—open or closed.^{4,13,15–18} Segmental ventilation models were integrated into segmental bio-heat models¹⁹ that modeled the thermal human response by simulating the changes in the skin and core temperature of the different body segments under different outside conditions affecting the state of thermal comfort.²⁰ This integration between the clothed cylinder ventilation model and the segmental

Department of Mechanical Engineering, Faculty of Engineering and Architecture, American University of Beirut, Beirut, Lebanon

Corresponding author:

Nesreen Ghaddar, Department of Mechanical Engineering, Faculty of Engineering and Architecture, American University of Beirut, PO Box 11-236, Riad El Solh, Beirut 1107 2020, Lebanon.
Email: farah@aub.edu.lb

bio-heat model succeeded in predicting local and overall sensible and latent body heat losses as well as segmental body thermal comfort.¹⁵

Other studies investigated the effect of limb swinging motion for a walking human in the presence of external wind using a clothed swinging finite cylinder model.^{11,12,14,21,22} Ghali et al.¹¹ and Ghaddar et al.¹⁴ addressed the effect of the changing gap width induced by an oscillating body part (cylinder) within a fixed single clothing cover at uniform external environment pressure, with closed and open clothing apertures. The developed swinging arm model of Ghaddar et al.¹⁴ and Ghali et al.¹¹ succeeded in estimating the renewal flow rates for general limb motion configuration. Their models were based on a 3D cylinder model, lumped in the radial direction due to a small air layer gap, and were shown to be accurate and robust, but they still necessitated significant computational cost. In addition, the inherent complexity of these models made it difficult to directly integrate them with segmental bio-heat models. For these reasons, the use of such detailed mathematical models by other researchers was limited.

Therefore, it is of interest to generate a simpler and robust ventilation model of a clothed walking human body to replace the complex models developed in the literature. This simplified model is considered as an interactive clothing design tool, having several advantages. First, such a simplified model is easily coupled with bio-heat models that simulate the human thermal response to predict thermal comfort in different applications. Second, the low computational cost of such a model facilitates the use of optimization to find the most effective clothing design. Third, the simplicity of the ventilation model makes it easier to be used by other researchers for different applications, for example, the use of the simplified model to estimate the ventilation rate afforded by the protective clothing to decrease the heat stress of the wearer.

On the other hand, developing an interactive tool for the estimation of static and dynamic clothing ventilation under wind and motion must be able to accommodate different wind conditions, different postures (standing or walking), and different clothing apertures (open or closed to environment). Furthermore, such a tool must be represented in a simple and conceptually understood method that captures, in the meantime, all the physics so as to be easily adopted and integrated with other models, such as the segmental bio-heat model. In this study, an analogy is adopted between the air flow inside the air gap and an electric circuit; this analogy has been widely used in the literature. Indeed, researchers have approached the problem of modeling the air flow in channels and complex geometries using an electrical circuit analogy^{23–25} because the electric circuit analogy is easily understood and

explained.²³ For example, Endo et al.²³ used the electric circuit analogy to model fluid permeation through a particle-packed non-uniform structure bed. Moreover, the analogy with an electric circuit is helpful in modeling the air flow through lungs where respiratory impedance is defined.²⁴ Akers et al.²⁵ reported the analogy between a laminar flow in a circular pipe subjected to a transient sinusoidal pressure difference and an electric circuit composed of inductance and resistance in series. In all these studies, the analogy is based on considering that the pressure difference and the flow rate are similar to the potential voltage difference and the electric current, respectively.²⁶ However, modeling clothing ventilation via electric circuit analogy has not been reported in the literature.

In this work, the pressure driven flow is studied in the microclimate air layer of the clothed human segment. This air flow is resisted by the viscous resistance inside the air layer and by a fabric resistance through the clothing layer. Moreover, if the clothed human segment is oscillating and the volume of air inside the microclimate air layer is changing, this will cause a variation in the air flow rate. Therefore, the analogy of the ventilation flow to the electric circuit is represented by an electric resistance describing the resistance to the air flow and by an electrical inductance describing the resistance to the change in air flow rate if oscillation occurs. The fluid flow expressions for resistance and inductance can be derived directly from the mathematical model, permitting the use of electrical circuits' analysis tools for their fluid analogies.

Therefore, in this study, a simplified model has been developed. This model is based on an analogy between the air flow inside the air gap and through the fabric with an electric circuit. The model considered different conditions of external wind and swinging motion of different clothed fabric segments representing the limb or the trunk. Furthermore, the model is validated by comparing the results with published papers under different conditions.

Research methodology

This study aims to develop a simplified ventilation model using an electric circuit analogy applied to the active or sedentary clothed human body segment (upper and lower limbs and trunk), with open or closed clothing aperture, and subject to external wind. In order to achieve this goal, the research methodology begins by developing an electric circuit model and solver for the air flow in the microclimate air layer between clothing and skin. The clothing ventilation is modeled as a pressure driven flow. Therefore, the equations of the model are converted to the simple equations of an electric circuit, where the pressure difference

is described by the voltage difference and the flow of air is analogous to the electrical current.

When air penetrates through clothing fabric, it is resisted by the clothing fabric, and then it moves angularly and axially. Within the microclimate, the air flow is resisted by a viscous resistance in the angular and axial directions. If the clothed segment is swinging due to walking, the volume of the air layer changes over a short period of time, which induces a change in the air flow rate. Therefore, the analogy between the pressure driven flow inside the microclimate air layer of the clothed segment and an electric circuit involves resistance and inductance elements. The electrical resistance is analogous to the resistance to air flow (viscous and fabric resistance), while the inductance designates the resistance to any change in the rate of the flow due to volume change. No capacitance element is used in the circuit since air in such an application is treated as an incompressible fluid, and clothing is treated as a rigid porous material, so that there is no storage of the flow. The resistance to the flow in each direction is denoted by a single value of a resistance, R , while the variation of flow induced by the variation of the air gap width in oscillating motion is impeded by the presence of inductance, L . Therefore, the analog electric circuit would be composed of a resistance with or without inductance in series as shown in Figure 1(a) and (b), respectively. In the clothed human trunk subject to external wind, no swinging motion occurs, therefore, the air gap width is not changing, which does not induce any change in the flow rate (no inductance). In this case, the pressure driven flow is analogous to an electric circuit composed of resistances only. In the clothed human limb case, if oscillation occurs, the pressure driven flow is analogous to a resistance-inductance (RL) electric circuit when the air gap width is changing, and is analogous to a resistance electric circuit when the air gap width is not changing.

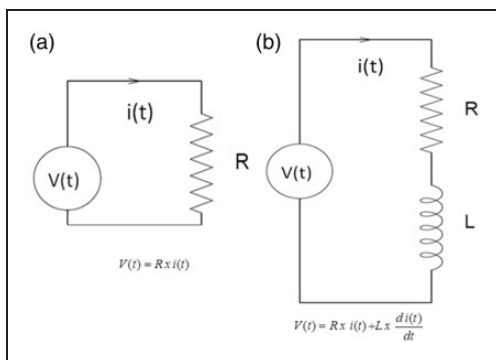


Figure 1. Electric circuit composed of (a) resistance only and (b) resistance and inductance in series

More information about the electric circuit is given in Appendix 2.

Finally, the validation of the proposed model will be done by comparison with published experimental data in which the trace gas method is used to estimate the ventilation for clothed segments.

Physical configuration

Figure 2(a) represents the upper human body parts composed of different segments. Each clothed segment is represented by a fabric covered cylinder, extensively used in the literature, as shown in Figure 2. ¹²⁻¹⁵ The fabric covered cylinder consists of two concentric cylinders of radii r and r_f , and height H (see Figure 2(b)). The microclimate air annulus of thickness $Y_0 = r_f - r$ is trapped between the inner solid cylinder maintained at temperature T_{skin} and the outer porous cylinder represented by an isotropic fabric layer of permeability α and thickness e_f . The top and the bottom ends of the annulus could be closed or open to the environment. The configuration could be subjected to an external air flow

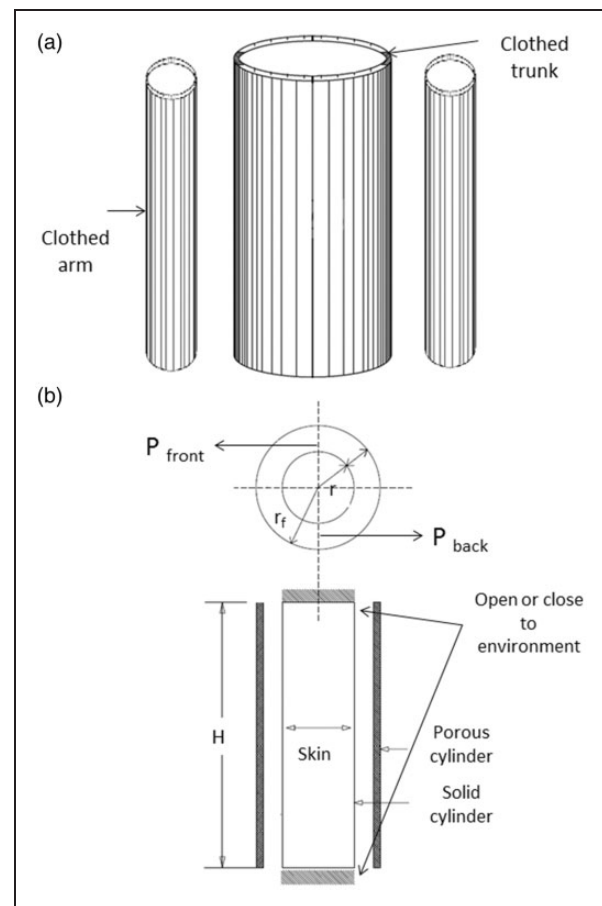


Figure 2. Physical configuration of (a) disconnected upper human body segments and (b) fabric clothed segment.

at a specific wind velocity v_w allowing air to enter through the permeable outer cylinder representing the fabric or the open aperture. Furthermore, the air flow could be induced by the oscillating motion of the clothed segment, representing the walking condition of the human body. In order to have a simplified model, each clothed segment (trunk or limb) is divided into two parts: one in front of the wind velocity and the other on the back side, as shown in Figure 2(b). Therefore, two pressures are defined in the microclimate air layer for each segment, and these pressures are P_{front} and P_{back} , reducing angular variation to lumped nodes.

Mathematical formulation

Electric circuit analogy in the case of clothed human trunk. In walking conditions, the clothed human trunk air gap size does not change with time because the trunk does not experience an oscillating motion when the human body is walking;¹⁴ however, the walking speed of the human body affects the relative wind. Therefore, the flow of air is only induced by the relative wind velocity, given by the following equation

$$v_r = v_w \pm v_{walk} \quad (1)$$

where v_w and v_r are, respectively, the wind speed and the relative wind.

The annulus trapped air thickness Y of the clothed trunk is relatively small compared to the height H and the inner radius cylinder r_s , which permits the following assumptions:⁴ (1) plane Poiseuille flow in axial and angular directions, (2) negligible variations of pressure in the radial direction. By integrating the angular and axial Navier–Stokes equations over the corresponding cross-section, the pressure difference equations of the trunk ($\Delta P_{t-axial}$, $\Delta P_{t-angular}$) are given as a function of the flow rate ($Q_{t-axial}$, $Q_{t-angular}$) by

$$\Delta P_{t-axial} = \frac{12\mu H_t}{Y_t^3(\pi r_t)} Q_{t-axial} \quad (2)$$

$$\Delta P_{t-angular} = \frac{12\mu(\pi r_t)}{Y_t^3 H_t} Q_{t-angular} \quad (3)$$

where Y_t , H_t , and r_t are, respectively, the air gap size, the height, and the radius of the trunk. Moreover, the air flow in the radial direction is through the permeable fabric covering the human body. The radial flow is penetrating or leaving through the fabric depending on the pressure difference between the outside and the microclimate air layer. Thus, the radial pressure difference ($\Delta P_{t-radial}$) is given as a function of the flow rate

($Q_{t-radial}$) by the following equation

$$\Delta P_{t-radial} = Q_{t-radial} \frac{\Delta P_m}{\alpha \pi r_t H_t} \quad (4)$$

where α is the air permeability of the fabric at the standard pressure $\Delta P_m = 124.5$ Pa.²⁷ On the other hand, given that the microclimate air layer is formulated as an incompressible fluid, the conservation of mass in the microclimate air layer of the clothed human trunk is given by

$$Q_{t-radial} + Q_{t-axial} + Q_{t-angular} = 0 \quad (5)$$

Equations (2), (3), and (4) are similar to the potential equation of the voltage difference across an electric resistance (see Figure 1 (a)). Indeed, the use of the resistance in the electrical circuit is logical because in the case of Poiseuille flow, the air flow rate is resisted by the viscous resistance, which depends linearly upon the air viscosity in polynomial dependence upon other geometrical properties (angular and axial directions). On the other hand, when going through a porous media, the air is resisted by an air resistance inversely proportional to the air permeability. Therefore, the analogy between the air flow inside the microclimate air gap of the trunk subjected to external wind in the axial, angular, and radial directions and the resistance electric circuit is reasonable. This analogy implies the definition of the resistances in the axial, angular, and radial directions as the following

$$R_{t-axial} = \frac{12\mu H_t}{Y_t^3(\pi r_t)} \quad (6)$$

$$R_{t-angular} = \frac{12\mu(\pi r_t)}{Y_t^3 H_t} \quad (7)$$

$$R_{t-radial} = \frac{\Delta P_m}{\alpha \pi r_t H_t} \quad (8)$$

In addition, equation (3) is similar to Kirchhoff's first law, and the network that is analogous to the air flow inside the microclimate air layer of the trunk is shown in Figure 3. The two parameters $P_{t-front}$ and P_{t-back} are, respectively, the pressures at the front side and the back side of the microclimate air layer of the clothed trunk. $P_{outside1}$ and $P_{outside2}$ are the pressures at the opening (if it is available) and outside the porous cylinder, respectively.²⁸ Therefore, the switch S_1 is opened if the top end of the clothed human trunk is open, and closed otherwise.

Electric circuit analogy in the case of a clothed human limb. During walking conditions, the human clothed

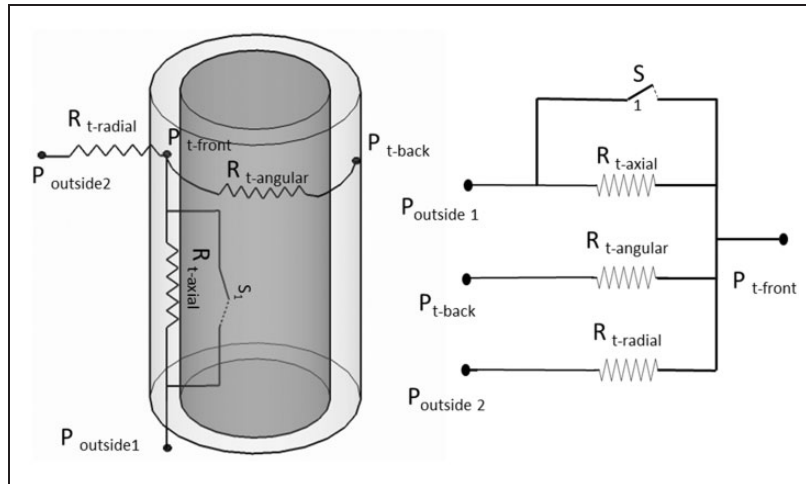


Figure 3. Network representing the analogy of the air flow inside the microclimate air layer of the clothed trunk subjected to external wind.

arm can be assumed to have a sinusoidal up and down (swinging) motion in contrast to the clothed trunk, which moves at the human walking speed without changes in microclimate air volume. The oscillating motion of the clothed arm is divided to two phases.¹⁴ In phase I, the human skin (inner cylinder) swings without touching the porous media (outer cylinder), forming an angle ϕ smaller than the angle at which contact occurs ($\phi_{contact}$) while, in phase II, the human skin and fabric swing together to a maximum angle ϕ_{max} . The various phases of the motion are demonstrated in Figure 4.

The contact angle is defined as a function of the initial microclimate air layer size of the arm (Y_{a-0}) to the arm height (H_a) as, follows

$$\phi_{contact} = \tan^{-1} \frac{Y_{a-0}}{H_a} \quad (9)$$

When the angle ϕ reaches $\phi_{contact}$, phase I terminates. During phase II, the skin touches the fabric and they swing together, reserving the same air layer thickness. In phase II, the maximum angle that the fabric and skin reach is ϕ_{max} . Therefore, a sinusoidal angular position ϕ can be assumed for the swinging motion at a rotational speed ω , related to the frequency of motion f as follows

$$\phi = \phi_{max} \sin(\omega t) \quad (10)$$

Therefore, the air layer thickness Y at any spatial position is given by¹⁴

- Phase I:

$$Y_a(x, \theta, t) = Y_{a-0} - (H_a - x) \tan \phi \cos \theta \quad (11)$$

- Phase II:

$$Y_a(x, \theta, t) = Y_{a-0} - (H_a - x) \tan \phi_{contact} \cos \theta \quad (12)$$

Because we are interested in developing a simplified one-dimensional (1D) model, the air gap size should be integrated in both the axial and angular directions, and the average is estimated. By integrating equation (11) and (12) over the front side angle ($-\pi/2$ to $\pi/2$) and the back side angle ($\pi/2$ to $-\pi/2$), and over the segment arm length H_a , and by considering that the oscillation angle ϕ is very small in Phase I as well as the contact angle $\phi_{contact}$, the equation of the air layer thickness Y becomes

- Phase I:

$$\bar{Y}_a(t) = Y_{a-0} - \frac{H_a}{\pi} \phi_{max} \sin(\omega t) \quad (13)$$

- Phase II:

$$\bar{Y}_a = Y_{a-0} - \frac{H_a}{\pi} \phi_{contact} \quad (14)$$

Therefore, the main difference between phase I and phase II is that the air gap size is changing with time in phase I, but is unchanged in phase II.

Phase I: air gap size changing with time. The annulus trapped air thickness Y of the clothed arm is relatively small compared to the height H and the inner radius cylinder r_a , which permits the following assumptions: (1) Womersley time-periodic laminar channel base flow

for the axial and angular directions^{12,13,29} in phase I, and (2) negligible variations of pressure in the radial direction in both phases. Thus, the velocity v has also a parabolic profile in the radial direction y given by

$$v(t, y) = k(y\bar{Y}_a(t) - y^2) \tag{15}$$

where k is a parameter ($m^{-1}\cdot s^{-1}$) which depends on a reference condition for velocity within the oscillation period in each direction (k_{axial} in the axial direction and $k_{angular}$ in the angular direction). By integrating over the corresponding flow cross-section, the air flow rates in the axial and angular direction are given, respectively, by

$$Q_{a-axial}(t) = k_{axial}\pi r_a \frac{Y_a^3(t)}{6} \tag{16}$$

$$Q_{a-angular}(t) = k_{angular}H_a \frac{Y_a^3(t)}{6} \tag{17}$$

The selected reference conditions are when the outer and inner cylinders are concentric (the microclimate air

layer gap is y_0), which occurs at $t=0$, $t=T/2$, and $t=T$ (see Figure 4). At these times, the reference volumetric flow rates in the axial and angular directions are, respectively, denoted as $Q_{a-0 axial}$ and $Q_{a-0 angular}$. Then, k_{axial} and $k_{angular}$ can be determined in the respective directions, and are given by

$$k_{axial} = 6 \frac{Q_{a-0 axial}}{\pi r_a Y_{a-0}^3} \tag{18}$$

$$k_{angular} = 6 \frac{Q_{a-0 angular}}{H_{a-s} Y_{a-0}^3} \tag{19}$$

The 1D momentum equations for microclimate air flow in axial and angular directions are given, respectively, by

$$x - direction : \rho \frac{\partial v_{axial}}{\partial t} = -\frac{\partial P_{a-axial}}{\partial x} + \mu \frac{\partial^2 v_{axial}}{\partial^2 y} \tag{20}$$

$$\theta - direction : \rho \frac{\partial v_{angular}}{\partial t} = -\frac{\partial P_{a-angular}}{R_{a-s}\partial\theta} + \mu \frac{\partial^2 v_{angular}}{\partial^2 y} \tag{21}$$

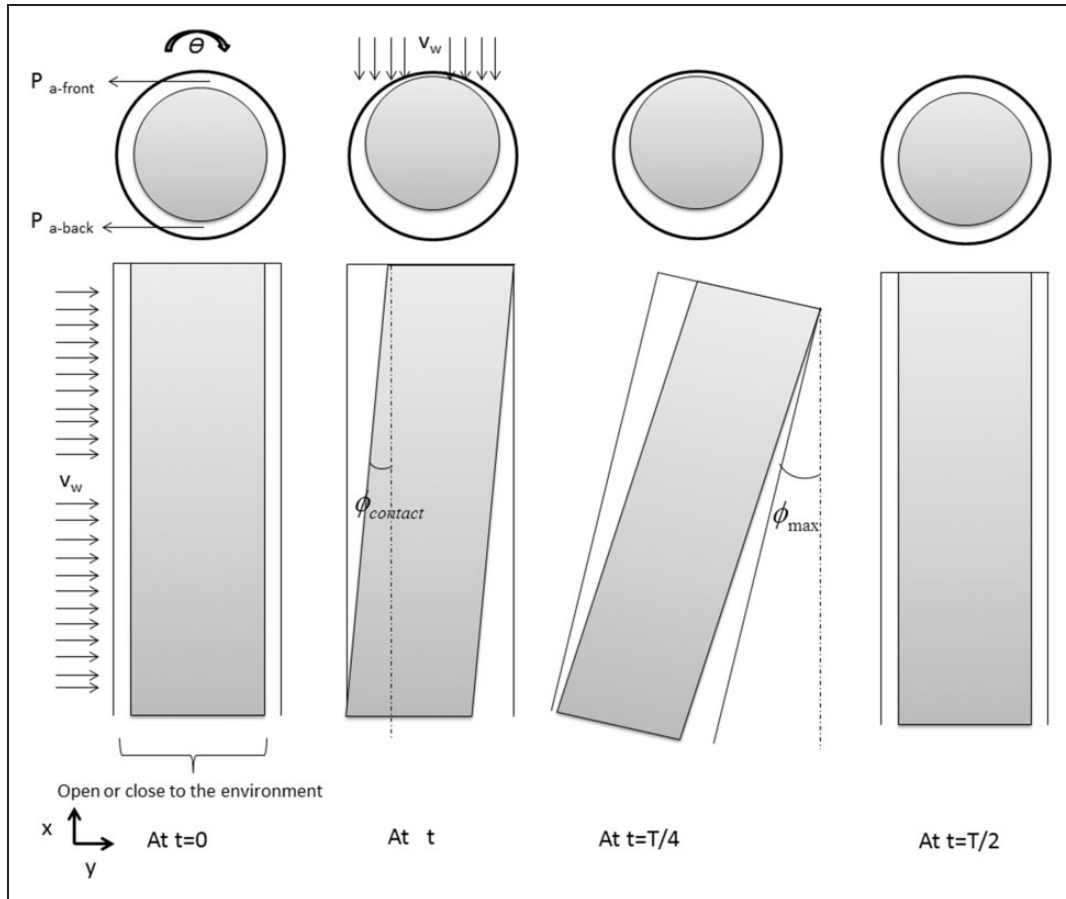


Figure 4. Physical configuration of the clothed human arm under oscillating motion and wind speed.

The derivative of the velocity given by equation (15) with respect to time is

$$\frac{\partial v(t, y)}{\partial t} = k y \left(-\frac{H_a}{\pi} \phi_{\max} \omega \cos(\omega t) \right) \quad (22)$$

The second derivative of the velocity given by equation (15) with respect to y is

$$\frac{\partial^2 v(t, y)}{\partial y^2} = -2ky \quad (23)$$

By integrating the momentum equations (21) and (22) over the corresponding cross-sections, the momentum equation in the axial and angular directions become, respectively

$$\begin{aligned} \rho r_a \int_0^y \int_0^\pi k_{axial} y \left(-\frac{H_a}{\pi} \phi_{\max} \omega \cos(\omega t) \right) dy d\theta \\ = -r_a \int_0^y \int_0^\pi \frac{\partial P_{a-axial}}{\partial x} dy d\theta - 2r_a k \mu \int_0^y \int_0^\pi y dy d\theta \end{aligned} \quad (24)$$

$$\begin{aligned} \rho \int_0^y \int_0^{H_{a-s}} k_{angular} y \left(-\frac{H_a}{\pi} \phi_{\max} \omega \cos(\omega t) \right) dy dz \\ = - \int_0^y \int_0^{H_{a-s}} \frac{\partial P_{a-angular}}{r_a \partial \theta} dy dz - 2k \mu \int_0^y \int_0^{H_{a-s}} y dy dz \end{aligned} \quad (25)$$

By substituting (16) and (17) in the integrated momentum equations above, the axial and angular pressure equations are developed as a function of the axial and angular flow rates, respectively, as

$$\Delta P_{a-axial} = \frac{12\mu H_a}{\bar{Y}_a^3 (\pi r_a)} Q_{a-axial} + \frac{\rho H_a}{\bar{Y} (\pi r_a)} \frac{dQ_{a-axial}}{dt} \quad (26)$$

$$\Delta P_{a-angular} = \frac{12\mu (\pi r_a)}{\bar{Y}_a^3 H_a} Q_{a-angular} + \frac{\rho (\pi r_a)}{\bar{Y}_a H_a} \frac{dQ_{a-angular}}{dt} \quad (27)$$

Moreover, the air flow in the radial direction flows over the permeable fabric covering the human body, and either penetrates into or leaves the air layer through the fabric, depending on the pressure difference between the outside air and the inside microclimate air layer. Thus, the radial pressure difference for the front half or back half of the annulus cylinder are given by

$$\Delta P_{a-radial} = Q_{a-radial} \frac{\Delta P_m}{\alpha \pi r_a H_a} \quad (28)$$

where α is the air permeability of the fabric at the standard pressure $\Delta P_m = 124.5 Pa$.²⁷

Equations (26) and (27) are analogous to the potential equation of the electric circuit shown in Figure 1(b), and are given by

$$V(t) = R i(t) + L \frac{di(t)}{dt} \quad (29)$$

The electric circuit is formed by a resistance and inductance in series. This analogy is reasonable because the Poiseuille air flow is resisted by the viscous resistance in the angular and axial directions on one hand, and on the other hand, the change of the air gap size induces a change in the air flow rate impeded by the presence of the inductance that is related to the density of the air and to the geometrical properties of the annulus. Therefore, we can conclude that there is an analogy between the air flow inside the microclimate air gap in both the axial and angular directions (subject to swinging motion and wind) and the resistance-inductance electric circuit. This analogy implies the following derived definition of the inductance and resistance in axial and angular direction

$$R_{a-axial} = \frac{12\mu H_a}{\bar{Y}_a^3 (\pi r_a)}, \quad L_{a-axial} = \frac{\rho H_a}{\bar{Y}_a (\pi r_a)} \quad (30)$$

$$R_{a-angular} = \frac{12\mu (\pi r_a)}{\bar{Y}_a^3 H_a}, \quad L_{a-angular} = \frac{\rho (\pi r_a)}{\bar{Y}_a H_a} \quad (31)$$

In addition, the air flow through the porous fabric in the radial direction given in equation (28) is similar to an electric circuit composed of a resistance only, as defined by

$$R_{a-radial} = \frac{\Delta P_m}{\alpha \pi r_a H_a} \quad (32)$$

Since air is treated as an incompressible fluid, the conservation of mass in the air layers implies that

$$Q_{a-radial} + Q_{a-axial} + Q_{a-angular} - r_a H_a \frac{dy}{dt} = 0 \quad (33)$$

Equation (33) is similar to Kirchhoff's first law, which states the principle of conservation of electric current, so that the algebraic sum of currents in a network meeting at a point is zero. Therefore, the electrical network representing the air flow inside the microclimate air layer of the clothed segment subject to external wind and oscillating motion and having an open connection to the environment is given in Figure 5, where $I_l = r_a H_a (dy/dt)$. The pressures $P_{a-front}$ and P_{a-back} are

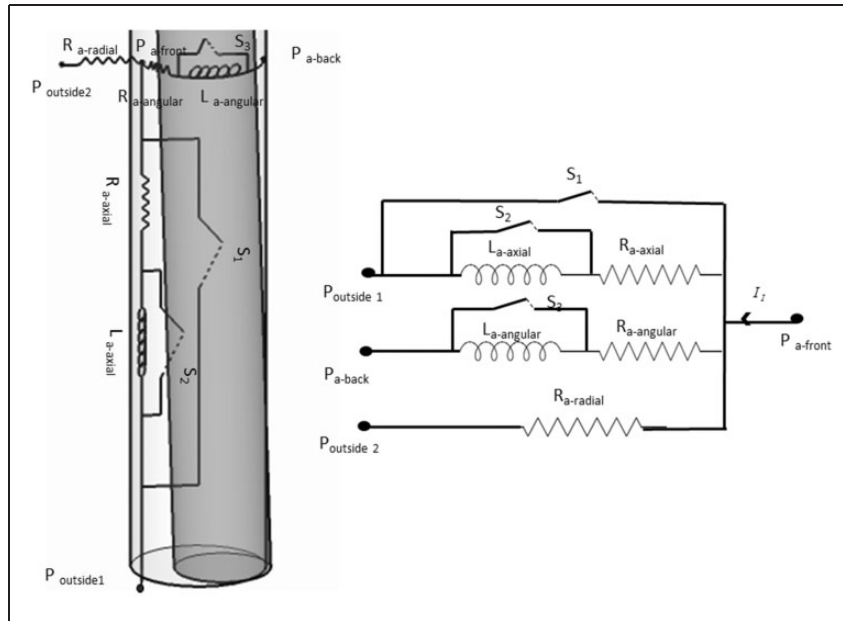


Figure 5. Network representing the analogy of the air flow inside the microclimate air layer of a clothed arm subjected to external wind and oscillating motion.

the pressures at the front side and the back side of the microclimate air layer of the clothed arm facing the wind, respectively. The pressures $P_{outside1}$ and $P_{outside2}$ are the pressures at the opening (if it is available) and outside the porous cylinder, respectively. The pressure $P_{outside2}$ is estimated from the data of Fransson et al.²⁸ on the pressure coefficient distribution around a circular cylinder with suction or blowing in the radial direction. It is worth noting that the amplitude of all the variables switch their signs when considering the governing equations on the back side. The main reason is that if the air gap size increases at a time t on the front side of the clothed segment, the back air gap size will decrease by the same amount at the same time t .

Phase II: air gap size unchanged with time. In phase II, the air gap size is unchanged with time and is given by equation (14). Therefore, the flow rates of equations in the axial, angular, and radial directions are not a function of time. By eliminating the transient term of equations (26), (27), and (33), the pressure difference equations become similar to the voltage equations across resistances defined by the same equations (30) and (31), while equation (33) is similar to Kirchhoff's first law without the transient term. Another important remark is that, during phase II, the angle formed is not relatively small, but is increasing from $\phi_{contact}$ to ϕ_{max} , thus a relative wind is produced and is given by

$$v_r = v_w \cos \phi \pm \frac{H_a}{2} \dot{\phi} \quad (34)$$

where v_w and v_r are, respectively, the wind speed and the relative wind. Therefore, in Phase II, the analogous network of the air flow is similar to the network of Figure 5, having closed switches S_2 and S_3 and having zero I_T , or, in the other words, it is similar to the clothed human trunk electric circuit of Figure 3 with different resistance values.

In summary, the model of air flow of the clothed human arm subjected to oscillating motion and wind is similar to the network shown in Figure 5, with open S_2 and S_3 switches in its first phase and closed S_2 and S_3 switches in its second phase. The S_1 switch opening and closure depends on whether the clothed arm presents an open aperture or not. If the clothed arm is open at the bottom end s , then the air flows axially through this opening; in this case, S_1 is opened, and vice versa.

Results and discussions

In this section, the model is validated by comparing the results of segmental and overall ventilation rates with published experimental data on clothing ventilation for different permeability, wind speed, oscillation frequency (for the clothed arm), walking conditions, and aperture configurations.^{8,10,14,29} For each case, all the inputs of the clothed segment were extracted from published experiments used for the comparison with predictions of the ventilation model.

Ke et al.⁸ used the tracer gas method to measure the local ventilation rates of the arm and trunk for different working garments. The experiment was based on injecting nitrogen gas (tracer gas) after pre-mixing it with air

into different locations in the garment. Then, the nitrogen concentrations were measured at the inlet and outlet using an N_2 analyzer. For each location, the microclimate ventilation rate was estimated using the tracer gas equation, and the average ventilation was reported for the local ventilation rate. Different conditions were examined: different garment permeability (0–0.135 m/s), different wind speeds (0, 0.6, and 0.9 m/s), and different aperture configurations (closed or open condition of the garment). The experiments were carried out in an air-conditioned chamber using a standing shop manikin.

Ke et al.¹⁰ investigated the local ventilation rates of an impermeable garment in two activities (static and walking) and two wind speeds (no wind and 1.2 m/s). The experiment was based on injecting argon gas (tracer gas) after pre-mixing it with air into different locations in the garment. They measured the argon concentrations at the inlet and outlet using a mass spectrometer, estimated the microclimate ventilation rate using the tracer gas equation for each location, and reported the average ventilation for the local ventilation rate. The experiment was carried out in an environmental chamber using a walking thermal manikin.

The third experiment was published by Ghaddar et al.¹⁴ to determine the ventilation induced by a swinging motion and external wind for a fabric covered cylinder representing a limb. Their experiment was conducted in a controlled environmental chamber using a permeable clothing fabric (0.05 m/s) tested at different wind speeds and oscillating frequencies. The periodic rotational motion of the inner cylinder was provided by a dc motor by means of a three-bar mechanism. The outer fabric cylinder rested on a thin metallic screen of 2 cm open squares where the cotton fabric was wrapped around and tightly fitted. The wind tunnel provided a laminar flow of air in front of the cylinder controlled by adjusting the rotational speed of the fan without compressing the fabric.¹⁴ They estimated ventilation rates using a tracer gas method (N_2 as a tracer gas). All of the above mentioned experiments measured the local ventilation rates of the upper human body segments.

The overall ventilation rate was validated using the published experiment of Ueda et al.³⁰ In their experiment, the overall ventilation rate was measured using a tracer gas technique tested on human subjects wearing a coverall of a specified air resistance (0.3 KPa.s/m) under the following conditions: standing still or walking at 1 m/s, in still air and in wind conditions at 1 m/s, for opened and closed suits. The effect of openings on the ventilation rates of the overall human body was also reported. The openings were located only on the collars and cuffs; no openings existed on the clothed legs.³⁰

Clothed trunk subject to wind

The published experimental data of Ke et al.⁸ are used for the validation of the model predictions of the ventilation rate of the clothed trunk subject to wind. The simplified model of the clothed trunk described in the section on the case of the clothed human trunk and its electrical analogy (see Figure 3) are adopted. The inputs to the simplified model are the geometrical dimensions, the air permeability of the fabric, the wind speed, the aperture configuration, and the walking speed. In this comparison, the trunk is static, thus the walking speed is zero. The height, radius, and air gap of the clothed trunk are, respectively, 65 cm, 14 cm, and 5 cm. When considering the opening aperture in the simplified model, the axial flow rate is included, and vice versa (switch S_I of Figure 3 is opened when the aperture is opened, and vice versa).

Figure 6 illustrates the comparison between the ventilation rates of the simplified model and the experiment performed by Ke et al.⁸ Although the maximum relative error between the experimental and the predicted ventilation rates was 30%, all the predicted ventilation rates were within the range of the standard deviation provided by Ke et al.⁸ Two reasons are behind this relatively large error. First, the standard deviation of the experiment used⁸ is large, and the relative error is estimated between the average experimental value and the predicted value of the ventilation rate. This large experimental standard deviation could be related to the measurement of the air permeability, the air gap size, or to the wind speed. Because the model developed is simplified, so it is sensitive to the input data. Indeed, a 10 % increase of air permeability results in increases of about 9 % and 8% for the trunk and arm ventilation rate, respectively. Moreover, a 10 % increase in air gap size results in an increase of about 5% for both the trunk and arm ventilation rates, noting that the air gap size is taken as constant in the model, which is not the case in the experiment for the thermal manikin used by Ke et al.^{8–10} On the other hand, a 10 % increase in the wind speed results in increases of about 8% and 6% for the trunk and arm ventilation rates, respectively. All these parameters affect significantly the standard deviation of the experiment. Second, the model assumes independent clothed segments, while according to Ke et al.⁹, air exchange between a specific garment and the environments includes also the air exchange between local body parts. No comparison was made between the experiment and the simplified model in the case of an impermeable garment when the aperture is closed (see Figure 6(a)), since in this case there is no way for the air to enter the microclimate layer. In their experiment, Ke et al.⁸ reported the ventilation rates at different wind speeds. They justified these finding by

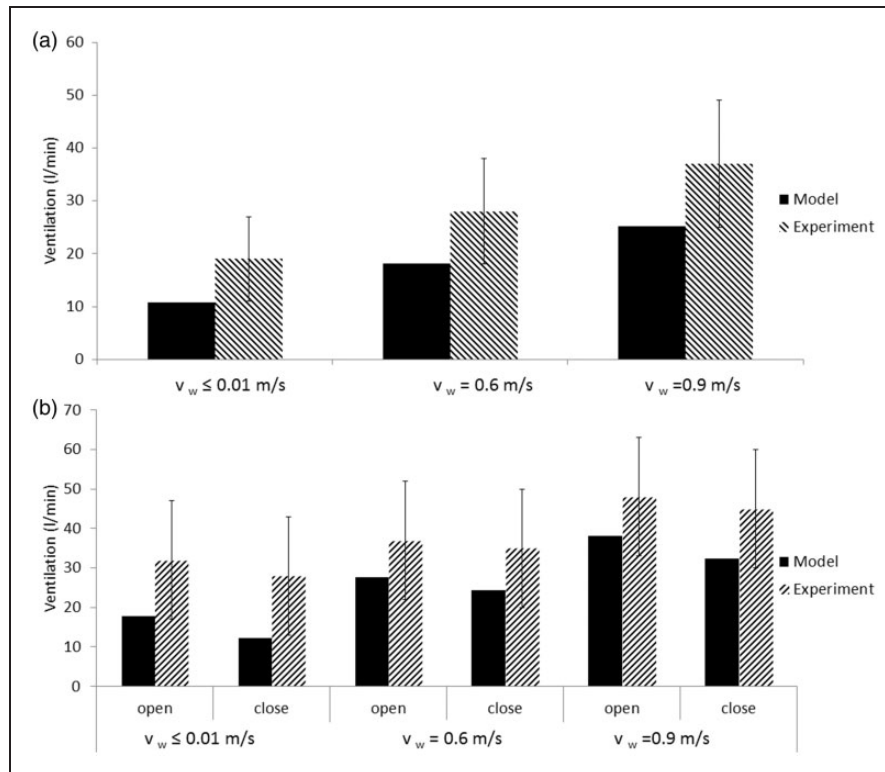


Figure 6. Comparison between the ventilation obtained by the simplified model and the published experiments⁸ for the clothed trunk at different wind velocity and aperture geometries for (a) impermeable open aperture and (b) permeable open and closed apertures.

stating that the opening cannot be totally closed experimentally; thus, their experimental results in this closed impermeable apertures were not applicable. The maximum ventilation rate is obviously attained at high permeability and wind speed (38 L/min) for the opening aperture. Figure 6(b) shows that an increase of 50% in wind velocity induces increases in ventilation rates of 44% for opened apertures compared to 33% for closed apertures. The reason behind these findings is that the pressure near the opening ($P_{outside1}$) increases with the increase of wind speed, thus, the pressure difference ΔP_{axial} increases, allowing more air to enter through the opening.

Clothed limb subjected to swinging motion and wind

Case of impermeable clothing. The published experimental data of Ke et al.¹⁰ are used for the validation of the model predictions of the ventilation rate of the impermeable clothed limb subject to oscillating motion and wind. The simplified model of the clothed arm subjected to oscillating motion and wind is thoroughly described in the section on the electric circuit analogy in the case of the clothed human limb. The analogy with the electric circuit presented in Figure 5 is adopted. The inputs to the oscillating arm model are the

geometrical dimensions of the clothed arm, the air permeability of the fabric, the wind speed, the aperture configuration, the oscillating frequency, and the oscillating amplitude. The height, radius, and air gap of the clothed arm are respectively 58 cm, 3.8 cm, and 1.6 cm. For the static activity, no oscillation is considered; thus, there is no change in air flow rate with respect to time (the switches S_2 and S_3 of Figure 5 are closed). For the walking condition, oscillation of the clothed arm occurs (the switches S_2 and S_3 of Figure 5 are open); thus the simplified model needs the oscillating frequency and the oscillating amplitude as inputs. The walking speed used in the experiment (1.25 m/s) corresponds to a frequency of about 80 r/min and a normal angle of oscillation $\phi_{max} = 20^\circ$. Another important input is the aperture configuration; in this section, the clothed arm is always open (switch S_1 of Figure 5 is open) because the garment is impermeable (closing the impermeable garment prevents air entering to ventilate the human body).

Figure 7 shows the comparison between the simplified model and the experiment ventilation rates at different conditions: walking with wind, walking without wind, and wind without walking. It is shown that all the predicted ventilation rates fall within the standard deviation range, with a mean relative error of 6%.

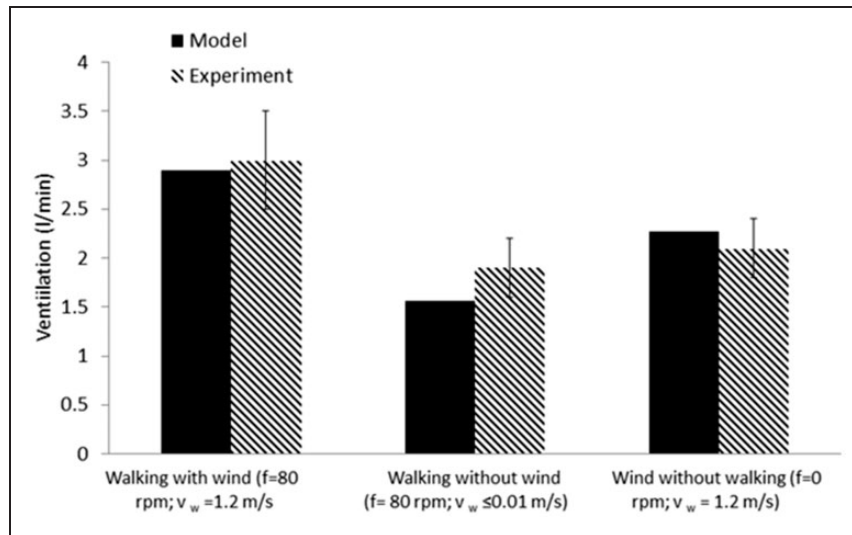


Figure 7. Comparison between the ventilation obtained by the simplified model and a published experiment¹⁰ for the impermeable clothed arm under different conditions (walking with wind, walking without wind, and wind without walking).

The condition of walking with wind presents the maximum ventilation (2.9 L/min) compared to other conditions. It is clear that walking in the direction of the wind will increase the relative wind velocity given by equation (34) which, in its turn, increases the pressure outside and induces more air to enter through the opening. The wind without walking condition comes in second place, with a ventilation rate of 2.2 L/min, exceeding that of the walking without wind condition (1.6 L/min) at approximately the same speed. This can be justified by the fact that when the oscillation of the arm is in the direction of the walking condition, the relative wind increases but the air layer gap decreases, affecting the ventilation rate in the opposite way.

It is worth mentioning that the under-estimation of the ventilation rate in the case of walking without wind could be related to the experiment: indeed, it is not possible to conduct an experiment in perfectly still air. Usually, in an indoor environment, and according to ASHRAE³¹ Standard 55-2010, the air speed is between 0.1 m/s and 0.2 m/s. So this could be the reason behind the under-estimation of the ventilation by the model. If we adjust the wind speed to 0.2 m/s in the model, the ventilation rate increases about 10% and approaches the experiment.

Case of permeable clothing. In this section, two published experiments are used. The first experiment is that of Ke et al.⁸, which reported measurements of the local ventilation rates of the arm for different wind speeds under a no walking condition (0 r/min). The second experiment is that of Ghaddar et al.¹⁴, which reported measurements of the local ventilation rates of the arm for different wind speed at different oscillation

frequencies (40–80 r/min). The combination of these two published experiments is achieved to permit study of the variation of the ventilation rates at different oscillating frequency (0–80 r/min). Therefore, the air permeability of the clothing must be the same in both experiment (0.05 m/s), as well as the wind velocity (0–1 m/s).

The simplified model of the clothed arm subjected to oscillating motion and wind is thoroughly described in the section on the electric circuit analogy in the case of the clothed human limb, where the analogy with the electric circuit presented in Figure 5 is adopted. The inputs to the oscillating arm model are the air permeability of the fabric (0.05 m/s), the wind speed (0–1 m/s), the aperture configuration (opened and closed), the oscillating frequency (0–80 r/min), and the oscillating amplitude ($\phi_{\max} = 20^\circ$). For the static activity (0 r/min), no oscillation is considered; thus, there is no change in air flow rate with respect to time (the switches S_2 and S_3 of Figure 5 are closed), and vice versa. Finally, the opening aperture induces a certain flow rate, and vice versa (switch S_1 of Figure 5 is opened when the aperture is opened, and vice versa).

Figure 8 illustrates the results of the ventilation rates through a permeable clothed limb ($\alpha=0.05$ m/s) for different frequencies and wind velocities, and shows that all the simplified ventilation results fall in the standard deviation range of the experimental results, with a maximum relative error of 18%. It is of interest to mention that the relative error provided by the detailed model of Ghaddar et al.¹⁴ was about 7%. Thus, although the proposed electric circuit analogous model is simplified, the relative error is, nevertheless, acceptable.

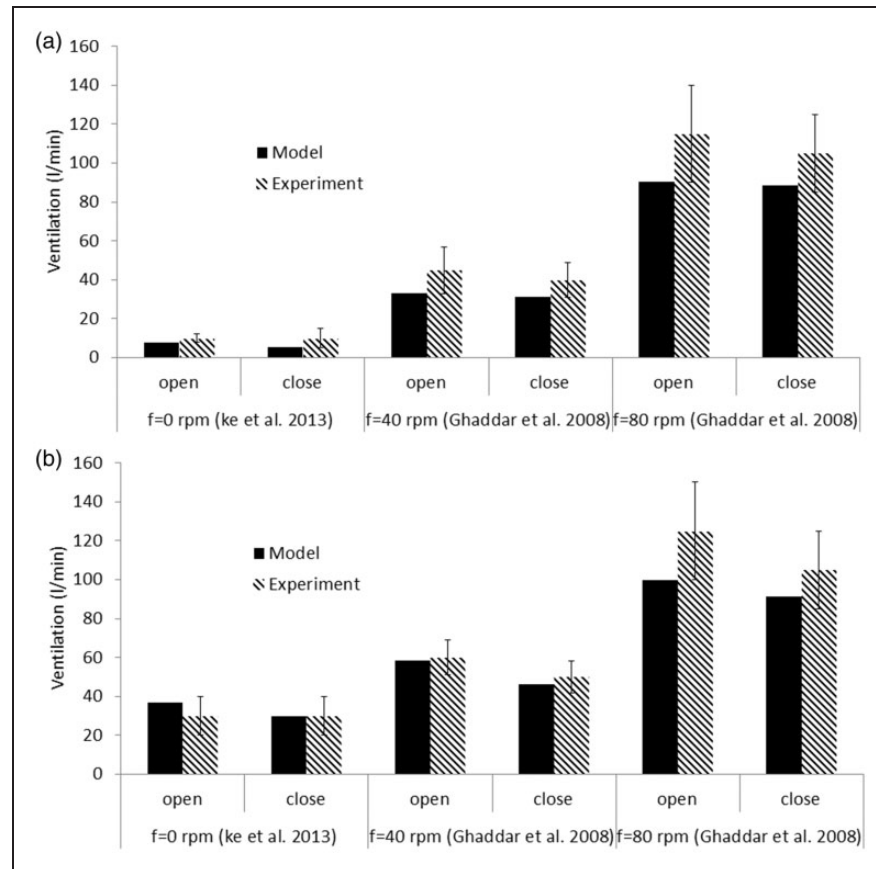


Figure 8. Comparison between the ventilation obtained by the simplified model and the published experiments^{8,14} for the permeable clothed arm at different frequencies and aperture geometries for (a) no wind speed, and (b) 1 m/s wind speed.

It is obvious that the maximum ventilation rate is attained in the case of high frequency oscillation (80 r/min) and high wind velocity for both opened (100 L/min) and closed apertures (91.4 L/min). The minimum ventilation rate is achieved for no-frequency and no wind speed (5 L/min) in the case of closed aperture. The reason is clearly that air cannot be exchanged because the opening is closed and the zero wind velocity is unable to create a significant pressure difference between the outside and the microclimate air layer that induces a flow through the permeable fabric. Another important remark is that increasing the oscillation frequency has a major effect for small wind speeds rather than large wind speeds. In fact, when the frequency doubles from 0 to 40 r/min, the ventilation triples in both open and closed apertures for the no-wind speed case, however; it only doubles at larger wind speed ($v_w=1$ m/s). This is related to the relative wind speed (equation (20)) profile, which shows that its variation with frequency attains its maximum at small wind speed. On the other hand, it is of interest to investigate the importance of opening aperture at different conditions. It is shown that the opening increases the ventilation rates of 25% at a frequency of 40 r/min,

while this increase decreases to 13% at a frequency of 80 r/min (for wind conditions). This means that when the frequency increases significantly, the opening's role in increasing the ventilation is reduced. This could be related to the period of pumping air through the opening in the oscillating condition. Indeed, as the frequency increases, the time of oscillation decreases, so that air does not have enough time to enter through the openings.

Finally, it is worth mentioning that in still air the oscillation induces a significant ventilation rate which increases with the oscillation frequency, to be comparable to the case of wind at high frequency. Therefore, a walking condition at high frequency could induce a significant ventilation rate in still air. However, this statement does not mean that walking in still air could cause thermal comfort because of the induced ventilation. The reason is that in the walking condition, the metabolic rate is higher, thus significant skin heat losses are needed to ensure thermal comfort. If the ventilation rate induced by the walking conditions is sufficient to relieve heat from the skin, the human body could sense thermal comfort in still air.

Overall clothing ventilation through permeable coverall

In this section, the overall ventilation rate is validated using the published experiment of Ueda et al.³⁰ The simplified model of the clothed trunk and clothed arm, presented, respectively, in the sections on the electric circuit analogy in the cases of clothed human trunk and of the clothed human limb, are both needed to calculate the overall ventilation rate. The ventilation rate of clothed legs is estimated based on the same strategy of the clothed trunk. The modeling of the clothed lower limbs was based on understanding of the human gait, which divides the motion cycle into the swing phase and the stance phase.³³ The swing phase of gait begins at toe-off, when the foot leaves the ground; the leg is then moved forward. The swing phase continues until the foot returns to the ground. Afterwards, the leg begins to support the body and this is called the stance phase. The sequence of swing and stance achieves one complete gait cycle.³³ For each leg, the swing phase occupies approximately 40% of the gait cycle, with 60% for the stance phase.³²

In the stance phase, the clothed leg is assumed vertical, because the angle that the knee forms with the vertical is almost zero.³³ In the swing phase, the clothed leg is deployed: the thigh goes forward while the calf goes backward. Although the knee angle attains 60°,³³ the increase in the relative wind speed on the thigh is

compensated by the decrease of the relative wind speed on the calf. For instance, when the knee angle was 60°, the relative wind speed on the thigh is approximately equal to the actual wind speed increased by 0.8 m/s. On the other hand, the calf experiences a relative wind speed equal to the actual wind speed decreased by 0.68 m/s. Therefore, the deflection of the clothed leg can be neglected. Moreover, in the swing phase, representing 40% of the gait cycle, two sub-phases occur: one for the no-touch and the other for the touch phase. The no-touch phase occupies a relatively small time of the swing phase; specifically, the no-touch phase ends when the knee touches the clothing. Therefore, this relatively small no-touch phase is considered negligible compared to the complete gait cycle. That is why the model does not consider the no-touch phase, and assumes that the ventilation rate of the clothed legs can be estimated based on the same strategy as the clothed trunk.

The air resistance of the coverall investigated (0.3 kPa·s/m) which is equivalent to an air permeability of 0.415 m/s at the standard pressure $\Delta P_m=124.5$ Pa (American Society for Testing and Materials, 1983). The inputs to the oscillating arm model are the air permeability of the fabric (0.415 m/s), the wind speed (0–1 m/s), the aperture configuration (opened and closed), the oscillating frequency corresponding to a walking speed of 1 m/s (65 r/min), the oscillating amplitude ($\phi_{\max} = 20^\circ$), and the geometrical dimensions

Table 1. Overall air exchange rate (min^{-1}) for a permeable coverall ($\alpha=0.415$ m/s) with closed and opened aperture in various conditions

		Closed Aperture			Opened aperture		
		Model	Experiment		Model	Experiment	
Still air ($v_w \leq 0.01$ m/s)	Standing	Left and right arm	0.5	2.8 ± 0.2	Left and right arm	0.56	3 ± 0.3
		Trunk	1.3		Trunk	1.4	
		Left and right legs	1.2		Left and right legs	1.2	
		Total	3		Total	3.16	
	Walking at $v_{\text{walk}} = 1$ m/s	Left and right arm	0.66	5.3 ± 0.3	Left and right arm	0.868	5.6 ± 0.1
		Trunk	2.48		Trunk	2.97	
Wind condition ($v_w = 1$ m/s)	Standing	Left and right arm	0.69	4.2 ± 0.3	Left and right arm	0.998	4.9 ± 0.5
		Trunk	2.48		Trunk	2.97	
		Left and right legs	1.71		Left and right legs	1.71	
		Total	4.88		Total	5.678	
	Walking at $v_{\text{walk}} = 1$ m/s	Left and right arm	1.16	6.3 ± 0.3	Left and right arm	1.32	6.6 ± 0.3
		Trunk	2.73		Trunk	2.89	
		Left and right legs	2.7		Left and right legs	2.7	
		Total	6.59		Total	6.91	

(same inputs as presented in the section on the clothed limb subjected to swinging motion and wind, case of impermeable clothing). The inputs to the oscillating trunk model are the air permeability of the fabric (0.415 m/s), the wind speed (0–1 m/s), the aperture configuration (opened and closed), the walking speed (1 m/s), and the geometrical dimensions (same inputs presented in the section on the clothed trunk subject to wind). The same inputs as the trunk model are used for the clothed legs, except for the geometrical dimensions (the height, radius, and air gap of the clothed legs are, respectively, 85 cm, 7 cm, and 4 cm). Finally, the experimental ventilation is given in air exchange rate per minute (min^{-1}); therefore, all the predicted ventilations are divided by the microclimate air layer volume (63 L).

The results of the comparison between the published experiment and the simplified model are shown in Table 1. Examining the data presented in Table 1, it is clear that all the predicted ventilation falls almost in the range of the standard deviation, with a maximum relative error of 14%. This could be related to the fact that the experiment is achieved without closing the connection between the trunk and the arm, while the model takes each clothed segment independently. Therefore, the discrepancy between the experiment and the model could be compensated by taking into account the interconnection between the trunk and the arm, as was reported by Ismail et al.^{34,35}

Conclusion

A study on the ventilation rate through clothing of the upper human body part segments has been developed. The periodic motion of the limbs subjected to different wind speeds has been illustrated during skin–fabric contact or no-contact for different aperture geometries. The ventilation through clothed trunk has also been estimated. The model derived from conservation laws was successfully transformed to an analog electric circuit for each case (limb and trunk). A comparison between the model results and different published experiments has been made and good agreement has been shown for the ventilation of different independent clothed segments. When considering the whole ventilation of the clothed human body, a maximum relative error of 14% has been shown. This could be the result of the opened interconnection between the trunk and the arm in the experiment. In further study, the model could be extended to consider the air flow inside the interconnection between the clothed arm and the clothed trunk by connecting the arm to the trunk model in one equivalent electric circuit.

Applications and further study

The developed simplified model can be used as an interactive optimization design tool in different clothing design applications for sports and warm climates. For instance, the simplified model can be integrated directly with segmental bio-heat models to simulate the human thermal response and thermal comfort of the wearer under different conditions and different body postures. Moreover, the ventilation model could be used to check for the performance of protective clothing against aerosol particles by comparing the ventilation afforded against the filtration rate. On the other hand, the simplified ventilation model could be integrated with a fabric model to properly estimate the ventilation rate through clothing, such as the three-node fabric model of Ghali et al.³⁶ Finally, the simplified model assumes a uniform air gap for the clothed segments.^{37,38} Therefore, it is of interest to improve the simplified ventilation model in order to account for the non-uniformity of the air gap by dividing the clothed segment into sub-segments with different air gap sizes.

Declaration of conflicting interests

The authors declared no potential conflicts of interest with respect to the research, authorship and/or publication of this article.

Funding

The authors disclosed receipt of the following financial support for the research, authorship, and/or publication of this article: This work was supported by the Lebanese National Council for Scientific Research for the project Award Number 103061-22909.

References

1. Birnbaum RR and Crockford GW. Measurement of the clothing ventilation index. *Appl Ergonom* 1978; 9: 194–200.
2. Havenith G, Ueda H, Sari H, et al. Required clothing ventilation for different body regions in relation to local sweat rates. In: *Proceedings of 2nd. European Conference on Protective Clothing: Challenges for Protective Clothing*, 21–24 May 2003, Switzerland: Montreux.
3. Ghaddar N, Ghali K and Chehaitly S. Assessing thermal comfort of active people in transitional spaces in presence of air movement. *Energ Buildings* 2011; 43: 2832–2842.
4. Ghaddar N, Ghali K, Al-Othmani M, et al. Experimental and theoretical study of ventilation and heat loss from isothermally heated clothed vertical cylinder in uniform flow field. *J Appl Mech* 2010; 77: 031011.
5. Crockford GW, Crowder M and Prestidge SP. A trace gas technique for measuring clothing microclimate air exchange rates. *Br J Ind Med* 1972; 29: 378–386.
6. Berglund LG and Akin FJ. Measurement of air exchange in diapers by tracer gas methods. *Tappi J* 1997; 80: 173–178.

7. Bouskill L, Havenith G, Kuklane K, et al. Relationship between clothing ventilation and thermal insulation. *J AIHA* 2002; 63: 262–268.
8. Ke Y, Havenith G, Li J, et al. A new experimental study of influence of fabric permeability, clothing sizes, openings and wind on regional ventilation rates. *Fiber Polym* 2013; 14: 1906–1911.
9. Ke Y, Havenith G, Zhang X, et al. Effects of wind and clothing apertures on local clothing ventilation rates and thermal insulation. *Text Res J* 2013; 0: 1–12.
10. Ke Y, Li J and Havenith G. An improved experimental method for local clothing ventilation measurement. *Int J Ind Ergonom* 2014; 44: 75–81.
11. Ghali K, Othmani M, Jreije B, et al. Simplified heat transport model of a wind-permeable clothed cylinder subject to swinging motion. *Text Res J* 2009; 79: 1043–1055.
12. Ghaddar N, Ghali K, Harathani J, et al. Ventilation rates of micro-climate air annulus of the clothing-skin system under periodic motion. *Int J Heat Mass Tran* 2005; 48: 3151–3166.
13. Ghaddar N, Ghali K and Harathani J. Modulated air layer heat and moisture transport by ventilation and diffusion from clothing with open aperture. *J Heat Tran* 2005; 127: 287–297.
14. Ghaddar N, Ghali K and Jreije B. Ventilation of wind-permeable clothed cylinder subject to periodic swinging motion: Modeling and experimentation. *J Heat Tran* 2009; 130: 091702.
15. Ismael N, Ghaddar N and Ghali K. Predicting segmental and overall ventilation of ensembles using an integrated bioheat and clothed cylinder ventilation models. *Text Res J* 2014; 0: 1–16.
16. Ghali K, Ghaddar N and Jones B. Empirical evaluation of convective heat and moisture transport coefficients in porous cotton medium. *J Heat Tran* 2002; 124: 530–537.
17. Lotens WA and Wammes LJA. Vapor transfer in two-layer clothing due to diffusion and ventilation. *Ergonomics* 1993; 36: 1223–1240.
18. Havenith G, Heus R and Lotens WA. Clothing ventilation, vapor resistance and permeability index: changes due to posture, movement and wind. *Ergonomics* 1990; 33: 989–1005.
19. Salloum M, Ghaddar N and Ghali K. A new transient bioheat model of the human body and its integration to clothing models. *Int J Therm Sci* 2007; 46: 371–384.
20. Ghali K, Ghaddar N and Bizri M. The influence of wind on outdoor thermal comfort in the city of Beirut: a theoretical and field study. *HVAC&R Res* 2011; 17: 813–828.
21. Ghaddar N, Ghali K and Jones B. Integrated human-clothing system model for estimating the effect of walking on clothing insulation. *Int J Therm Sci* 2003; 42: 605–619.
22. Ghali K, Ghaddar N and Jones B. Modeling of heat and moisture transport by periodic ventilation of thin cotton fibrous media. *Int J Heat Mass Tran* 2002; 45: 3703–3714.
23. Endo Y, Ngan CL, Nandiyanto AB, et al. Analysis of fluid permeation through a particle-packed layer using an electric resistance network as an analogy. *Powder Technol* 2009; 191: 39–46.
24. Ionescu CM and De Keyser R. Relations between fractional-order model parameters and lung pathology in chronic obstructive pulmonary disease. *IEEE Trans Biomed Eng* 2009; 56: 978–987.
25. Akers A, Gassman M and Smith R. *Hydraulic power system analysis*. Boca Raton, FL: CRC Press, 2006.
26. Oh KW, Lee K, Ahn B, et al. Design of pressure-driven microfluidic networks using electric circuit analogy. *P Soc Photo-opt Ins* 2012; 12: 515–545.
27. ASTM D737-75. Standard Test Method for Air Permeability of Textile Fabrics, (IBR) approved 1983.
28. Fransson JHM, Konieczny P and Alfredsson PH. Flow around a porous cylinder subject to continuous suction or blowing. *J. Fluids Struct* 2004; 19: 1031–1048.
29. Womersley JR. Oscillatory motion of viscous liquid in thin-walled elastic tube: i. The linear approximation for long waves. *Phil Mag* 1955; 46: 199–221.
30. Ueda H and Havenith G. The effect of fabric air permeability on clothing ventilation. In: Tochihara Y and Ohnaka T (eds) *Environmental Ergonomics*. Vol 3, Elsevier: Amsterdam, 2005, pp.343–346.
31. ASHRAE Standard 55-2010. *Thermal Environmental Conditions for Human Occupancy*. Atlanta, GA: American Society of Heating, Air-Conditioning and Refrigeration Engineers, Inc., 2010.
32. Mena D, Mansour JM and Simon SR. Analysis and synthesis of human swing leg motion during gait and its clinical applications. *J Biomechs* 1981; 14: 823–832.
33. Yamamoto H. The change in knee angle during the gait by applying elastic tape to the skin. *J Phys Ther Sci* 2014; 26: 1075.
34. Ismail N, Ghaddar N and Ghali K. Effect of inter-segmental air exchanges on local and overall clothing ventilation. *Text Res J* 2016; 86: 423–439.
35. Ismail N, Ghaddar N and Ghali K. Improving local ventilation prediction by accounting for inter-segmental ventilation. *Text Res J* 2016; 0: 1–17.
36. Ghali K, Ghaddar N and Jones B. Multi-layer three-node model of convective transport within cotton fibrous medium. *J Porous Media* 2002; 5: 17–31.
37. Roberts M, Jamriska M, Skvortsov A, et al. *Study on aerosol penetration through clothing and individual protective equipment (No. DSTO_TR_2283)*. Melbourne, Victoria: Defense Science and Technology Organization Victoria (Australia), Human Protection and Performance Division, published by Commonwealth of Australia, 2009.
38. Ghaddar N, Ghali K and Jones B. Convection and ventilation in fabric layers. In: Pan N and Gibson P (eds) *Thermal and moisture transport in fibrous materials*. Cambridge: Woodhead Publishing, 2006, Ch. 8, pp.271–307.

Appendix I

Notation

e_f thickness of the outer cylinder representing the fabric (m)

f	walking frequency (Hz)
H	cylinder length (m)
i	electric current (A)
k	parameter ($\text{m}^{-1}\cdot\text{s}^{-1}$)
L	electric inductance
Q	volumetric flow rate (m^3/s)
P	pressure (Pa)
R	electric resistance
r	radius of the inner cylinder representing the human body skin (m)
r_f	radius of the outer cylinder representing the fabric (m)
t	time (s)
T	temperature ($^{\circ}\text{C}$)
V	voltage (V)
v	velocity (m/s)
v_r	relative wind velocity (m/s)
v_w	wind velocity (m/s)
v_{walk}	walking velocity (m/s)
x	axial position
y	radial direction
Y	microclimate air layer size (m)
\bar{Y}	average microclimate air layer size (m)
ΔP	pressure difference (Pa)
ΔY	microclimate air gap amplitude (m)
α	permeability of fabric ($\text{m}^3/\text{m}^2\cdot\text{s}$)
θ	angular direction
μ	dynamic viscosity ($\text{kg}/\text{m}\cdot\text{s}$)
ρ	density of air (kg/m^3)
ϕ	oscillation angle
ω	angular frequency (rd/s)

Subscripts

0	initial condition
a	arm
axial	axial direction
angular	angular direction
back	back side
contact	contact
front	front side
max	maximum
outside 1	ambient side at the opening aperture
outside 2	ambient side around the porous cylinder
radial	radial direction
skin	skin
t	trunk

Appendix 2: Electric circuit description

Electric resistance

An electric resistance is an electronic component that resists the flow of electric current in an electric circuit. The electric resistance is analogous to the thermal resistance in heat transfer and to friction in a mechanical system. In this study, it is similar to the viscous resistance against the flow of air in the microclimate air layer, and to the fabric resistance against the flow of air through clothing.

Electric inductance

An inductor is an electronic component composed of a coil of wire that resists the change of current in an electric circuit. In this study, the flow of air, similar to the flow of current, is changing because the volume of the air gap is changing. Thus the resistance to the change of the air flow is described by the electronic inductance.

Resistance circuit and resistance-inductance circuit

When a difference in voltage is applied across an electronic resistance, a flow of electric current occurs and is resisted by the electronic resistance. According to Ohm's law, the resistance is equal to the voltage divided by current ($R = V/I$) where R is resistance, V is voltage and I is current. When a difference in voltage is applied across an electronic inductance, the inductance opposes the change of the electric current. The inductance L is equal to $V/(dI/dt)$ where V is Voltage, I is current, and t is time.

In an electric circuit, when the resistance and inductance are put in series, the voltage across the electronic devices is summed. Thus, in a resistance-inductance circuit, the voltage is given by

$$V = RI + LdI/dt \quad (35)$$